



Available online at www.sciencedirect.com

ScienceDirect

journal homepage: www.elsevier.com/locate/bbe



Original Research Article

A novel approach for segmentation and counting of overlapped leukocytes in microscopic blood images



K. Sudha^{*}, P. Geetha

Department of Computer Science and Engineering, College of Engineering, Anna University, Guindy, Chennai, India

ARTICLE INFO

Article history:

Received 19 August 2019

Received in revised form

10 January 2020

Accepted 13 February 2020

Available online

Keywords:

Leukocytes

Microscopic blood images

Edge strength

Grabcut technique

Gradient circular hough transform

ABSTRACT

Leukocytes count in the blood smear images plays an important role in identifying the overall health of the patient. The major steps involved in leukocytes counting system are segmentation and counting. However, the counting accuracy is greatly affected due to the morphological diversity of cells, the presence of staining artifacts and the overlapped cells. Therefore, this paper introduces a new framework to segment and counting of leukocytes. To segment leukocytes, an edge strength-based Grabcut method has been proposed. Later, the leukocyte region including the overlapped cells was counted using the novel gradient circular hough transform (GCHT) method. The research work was performed on ALL-IDB and Cellavision datasets. The proposed segmentation method has yielded high precision, recall and *f*-measure compared to the state-of-the-art methods. Additionally, comparison analysis was performed between the region count obtained using the existing and the GCHT method. The overall experimental results of the work showed that the proposed framework produced more accuracy in counting the leukocytes.

© 2020 Nalecz Institute of Biocybernetics and Biomedical Engineering of the Polish Academy of Sciences. Published by Elsevier B.V. All rights reserved.

1. Introduction

Leukocytes or white blood cells (WBCs) constitute a part of the immune system. Leukocytes are divided into five types: monocytes, lymphocytes, neutrophils, eosinophils and basophils. Leukocytes counting is used to detect abnormalities in patients. Leukocytes counting under microscope is highly dependent on the pathologist skills. It increases the operator burden and also is a time-consuming task. The WBC counting system consists of two stages: segmentation and counting.

However, effective leukocyte segmentation has been found to be a challenging task due to image quality, poor contrast and morphological variations in cells. However, due to overlapped WBC cells, the counting accuracy is low. This research work aims to design a system to accurately segment the leukocytes and also count the overlapped cell regions in the blood smear image.

Many authors attempt to achieve better segmentation results for counting analysis. Sajjad et al. [1] used the colour k-means algorithm to extract leukocytes from the microscopic blood images. The overall segmentation accuracy of their proposed method is found to be 94.3%. Ghane et al. [2]

^{*} Corresponding author at: Department of Computer Science and Engineering, College of Engineering, Anna University, Guindy, Chennai, India.

E-mail addresses: sudhak1691@gmail.com (K. Sudha), P.Geethageethapalanisamy@annauniv.edu (P. Geetha).

<https://doi.org/10.1016/j.bbe.2020.02.005>

0208-5216/© 2020 Nalecz Institute of Biocybernetics and Biomedical Engineering of the Polish Academy of Sciences. Published by Elsevier B.V. All rights reserved.

proposed an unsupervised k-means clustering that was utilized to segment WBC nuclei in blood smear images. For segmentation, the authors have got a precision of 96.07%. Negm et al. [3] used the k-means clustering to identify the leukemia cells. This method demonstrated an overall accuracy of 99.517%. In [4], the authors applied a k-means with morphological operations to extract leukocytes. The authors achieved a precision up to 98.35%. Zheng et al. [5] used the k-means clustering to segment WBCs from microscopic images. Cao et al. [6] proposed a k-means clustering to segment bone marrow cells in blood smear images. The authors achieved an average segmentation accuracy of 91.76%. Therefore, the k-means algorithm needs to be fine-tuned to resolve the problems related to cluster initialization. Significant improvement of precision values is needed.

Rawat et al. [7] proposed an Otsu's threshold to identify nucleus in blood smear images. Effective segmentation results were achieved by the author. Mishra et al. [8] used the triangle thresholding to segment leukemia cells from blood smear images. The authors delivered appreciable accuracy of leukocytes segmentation. Hegde et al. [9] formulated a robust algorithm based on Otsu threshold to segment WBC nuclei from the background. The segmentation accuracy is found to be 99%. Wang et al. [10] proposed an Otsu's histogram thresholding method to leukocyte nucleus in blood smear images. The thresholding technique necessitate tuning to produce fine segmentation results, which could have been upgraded or minimized. Rawat et al. [11] designed a Chan-Vase level set method to extract WBCs from blood smear images. Overall segmentation accuracy was reported to be around 98.7%. Moshavash et al. [12] used the intuitionistic fuzzy divergence based thresholding to segment leukocytes. Supriyanti et al. [13] proposed a template matching method to segment leukocytes from microscopic blood images. The study reported the use of 5 images and achieved average accuracy. Wang et al. [14] proposed a mathematical morphology-based method to detect WBCs from the background and reported segmentation accuracy of more than 90%. Chaira [15] used the intuitionistic fuzzy set to detect WBCs. The authors achieved average segmentation accuracy using 100 pathology images. Duan et al. [16] designed a robust algorithm to detect the WBCs from hyperspectral images. Cao et al. [17] designed a location-based grabcut algorithm to segment leukocytes in microscopic blood images and reported f -measure 0.9346. Liu et al. [18] used the adaptive location iterative grabcut method to detect leukocytes in blood smear images. They reported the precision to be around 0.9449. Since the morphological variations of WBC and presence of artifacts, it is difficult to achieve accurate segmentation results of blood smear images. If the leukocyte segmentation is unreasonable, then the counting cannot be achieved as well.

Safuan et al. [19] proposed an Otsu's thresholding method to detect WBCs from the background and circular hough transform (CHT) for counting analysis. The authors have got a counting accuracy of 96.62%. Wang et al. [20] proposed a WBC nucleus segmentation method based on the color component difference. The B-G values used to segment the leukocyte nuclei-based on thresholding method. They achieved better counting results using the proposed method. In [21], the

authors used a new and fully automatic proliferation index estimation (FLAPIE) algorithm to detect immunopositive and immunonegative nuclei in the DAB and H stained sample. The adaptive thresholding was performed separately in DAB and H stained images to remove small dark brown spots and bright blue artifacts in stained cell membranes. Wang et al. [22] proposed an object detection task and applied two object detection methods for leukocyte recognition. They achieved accuracy of 90.09% with running time 53 ms. Fan et al. [23] used the R-convolutional neural network (CNN) mask to localize and segment leukocytes from the background. Zhao et al. [24] proposed the method that detects WBCs from the microscope images based on the relationship between colours and the morphological operations. In [25], the authors designed automatic machine learning approach able to perform image segmentation for counting analysis. Ruberto et al. [26] used the thresholding method to segment leukocytes for differential counting analysis. Porcu et al. [27] proposed a method to segment WBCs nuclei by using vector field convolution (VFC) and to separate potential clumps watershed transform. But, the major challenge in counting techniques since the overlapped WBCs present in blood smear images. For the WBCs counting, it is essential to consider the overlapped WBC regions to achieve high accuracy outcomes. Therefore, a novel edge strength-based grabcut with new GCHT method for counting analysis has been proposed in this paper. The main contributions of this framework are described as follows:

- The edge strength-based Grabcut approach for leukocytes segmentation in microscopic blood images has been proposed.
- A novel GCHT algorithm has been proposed for overlapped WBC region counting in blood smear images.
- The proposed framework has been validated on the ALL-IDB and Cellavision datasets.
- Finally, comparative counting analysis using the GCHT technique and existing methods has been performed.

The paper has been organized as follows: Detailed description of the proposed framework is given in Section 2. Datasets and evaluation parameters used in this research work are described in Section 3, and Section 4 shows the experimental results. Section 5 discusses the key findings and Section 6 concludes the paper.

2. Methodology

The block diagram of the proposed framework is shown in Fig. 1. The proposed approach consists of four main stages: (1) HSV color conversion; (2) Edge strength-based location detection; (3) Fine segmentation using Grabcut approach; (4) WBCs counting using proposed GCHT method.

2.1. Color conversion

The input RGB image is first transformed to an HSV image. The work was carried out on the S component after extracting the S component separately since the S component contains more leukocyte information in microscopic blood images.

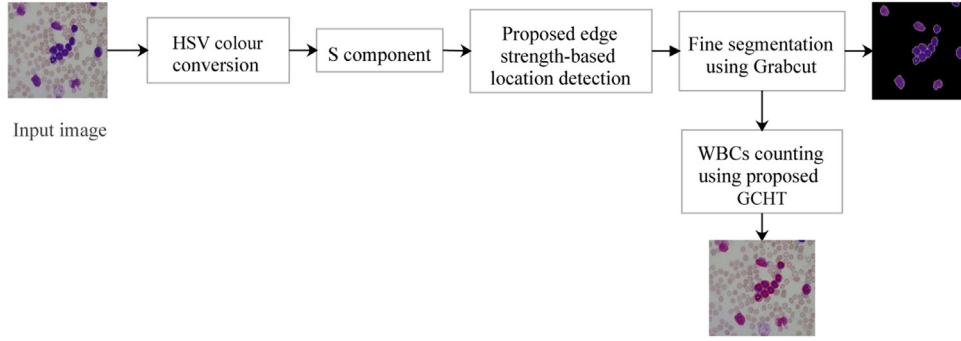


Fig. 1 – Block diagram of the proposed methodology.

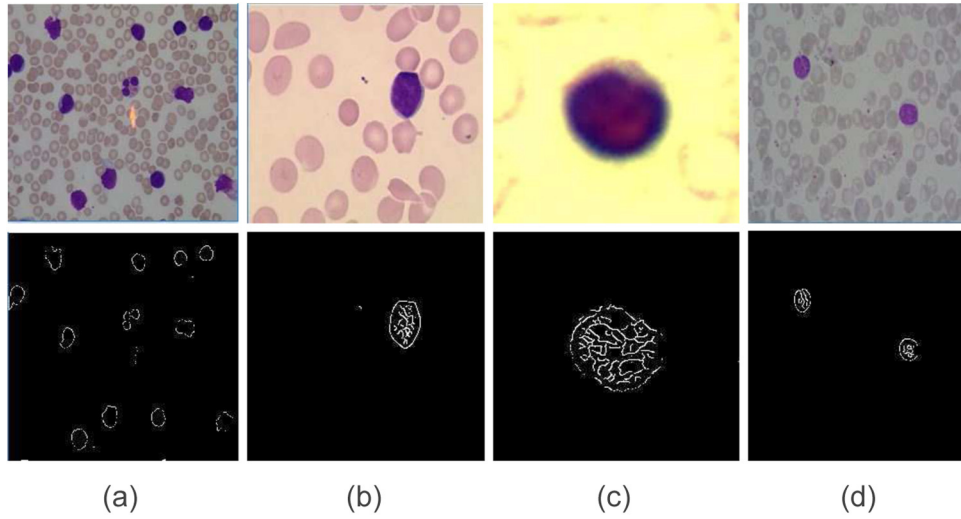


Fig. 2 – Examples of WBC edge pixels extraction using threshold ($T = 110$) for four different datasets. a ALL-IDB. b Cellavision. c Cell image [28]. d MUI dataset.

2.2. Proposed edge strength-based location detection

The best way of finding edge strength is the gradient magnitude $M(x, y)$ of an image $G(x, y)$ and direction (x, y) of each pixel of the leukocytes were calculated as follows:

$$M(x, y) = \sqrt{G_x(x, y)^2 + G_y(x, y)^2} \quad (1)$$

where $G_x(x, y)$ and $G_y(x, y)$ are the horizontal and vertical gradients, respectively.

Then, binary image $B(x, y)$ was computed as follows,

$$B(x, y) = \begin{cases} 1, & M(x, y) > T_1 \\ 0, & \text{otherwise} \end{cases} \quad (2)$$

where ($T_1=110$) is the threshold value, which was chosen based on the highest percentile in the intensity scale range [0–255].

Leukocytes pixels have high intensity values than other objects such as platelets and red blood cells (RBCs). The highest percentile is used to select high intensity WBC pixels. Illustration of WBC edge pixels extraction using highest percentile for four different datasets is shown in Fig. 2. Next, the marker image from input image $G(x, y)$ and binary image $B(x, y)$ was computed using Eq. (3)

$$N(x, y) = G(x, y) \cdot B(x, y) \quad (3)$$

where \cdot denotes the product of two images. This marker image used to select pixels from $G(x, y)$ corresponds to strong WBC edge pixels. Further, histogram using only the pixels in $G(x, y)$ that correspond to the locations of the 1-valued pixels in $B(x, y)$ was computed. Later, the threshold ($T_2 = 0.75$) was computed, which is approximately midway between the peaks in the histogram. Fig. 3 shows the steps to find WBC edge pixels. Further, $T_2 = 0.75$ was applied to gradient image $M(x, y)$ to

retain edges in WBCs and other edges were removed. If the edge magnitude is higher than threshold, it is assigned as a possible WBC edge point. The decision rule is given as

- If $M(x, y) > T_2$, then WBC edge point else non-WBC edge point.

Algorithm 1. Proposed Edge Strength Location Detection

```

Algorithm 1: Proposed Edge Strength Location Detection
Input : Input image  $f(x, y)$ 
Output: Set of location windows  $f_{box}$ 

1 begin
2   for each  $f(x, y)$  do
3     Perform HSV conversion
4     Extract S component separately
5     Find magnitude  $M(x, y)$  on S component using Eq. (1)
6     if  $M(x, y) > T_1$  then
7        $B(x, y) = 1$ 
8     else
9        $B(x, y) = 0$ 
10    end
11    Compute marker image from  $f(x, y)$  and  $B(x, y)$  using Eq. (3)
12    Construct histogram of marker image.
13    Find threshold from computed histogram ( $T_2 = 0.75$ )
14    Find the WBC edge pixels
15    if  $M(x, y) > T_2$  then
16      Detect WBC edge point
17    else
18      Remove non-WBC edge point
19    end
20  end
21  Compute location windows  $f_{box}$ 
22 end

```

Later, the red windows were computed on the obtained binarized image using the bounding box property in MATLAB. Fig. 4(a) shows the input image and Fig. 4(b) shows the location windows with the highest edge magnitude and Fig. 4(c) shows the WBCs location windows. Algorithm 1 represents the steps of proposed WBCs location detection.

2.3. Fine segmentation using Grabcut method

In [29], the initial information about the foreground and the background of an object was given by the user as a rectangular box around the object. Pixels outside the box were known background and the pixels inside were marked as unknown. From this information, a method that can be used to determine if the unknown pixels are either foreground or background of an object can be created. The proposed edge strength location windows are taken as an input of the Grabcut method. The following were the important information of the Grabcut method (Fig. 4).

- The Grabcut algorithm consists of two parts. The first part describes how much each pixel, x and y , is connected to its neighbourhood and is calculated using Eq. (4)

$$N(x, y) = \frac{\gamma}{\text{dist}(x, y)} e^{-\beta \|z_x - z_y\|^2} \quad (4)$$

$$\beta = \frac{1}{2(\|z_x - z_y\|^2)} \quad (5)$$

where z_x and z_y represent pixels of an image and $\gamma = 50$. The $\text{dist}(x, y)$ is the Euclidean distance of neighbourhood pixels.

- The second part contains pixels that have two nodes such as the background and foreground node. The links between the

nodes and pixel were denoted as $L(m)$.

$$L(m) > \sum_{n=1}^{\infty} N_n(x, y) \quad (6)$$

$$L(m) = 8\gamma + 1 \quad (7)$$

2.4. Proposed gradient circular hough transform

Microscopic blood images will have overlapped WBC regions. The ALL-IDB dataset also contain touching WBC regions in images. Accurate counting results cannot be achieved if touching cell regions are not separated. Many authors attempted to separate the overlapped WBC regions for counting analysis. Therefore, a new method had to be devised to solve this problem. Therefore, we have proposed the novel GCHT method to count touching WBC regions in smear images even though cells not separated. Moreover, the proposed framework does not require any algorithm to separate touching cells. The GCHT method is able to separate and count the overlapped cell regions with minimal complexity. The GCHT algorithm determines the best intersection points using Eqs. (8) and (9) given below, where a and b are defined as the centre of the circle. X_1 and Y_1 will give the parameter of the circle, θ is the angle through 360° and r_c is circle's radius.

$$X_1 = a + r_c \cos \theta \quad (8)$$

$$Y_1 = b + r_c \sin \theta \quad (9)$$

The GCHT procedure was as follows:

- The centroid values were obtained for each WBC in the smear image. Then, the distance of boundary pixels from the centroid was determined.
- The minimum and maximum distance values were recorded in an accumulated array. The radius range was set by the minimum and maximum values obtained from the array.
- The GCHT was based on the gradient field of the input smear image. A thresholding on the gradient magnitude is performed before the voting process of the GCHT to remove the uniform intensity.
- The pixel with a gradient magnitude smaller than the gradient threshold was not considered in the further computation.
- Generally, the gradient threshold value was chosen with a maximum intensity range [0-255]. Hence, the gradient threshold value set to 0.75 and it was given as input to suppress the false positives.
- The gradient threshold was obtained from the histogram of non-zero strong WBC edge pixels in Section 2.2. The GCHT method operates by drawing circles that fall within the specified radius range.
- The circles in the smear image had small irregularities along the edges, which could lead to an accumulation array that was bad for local maxima detection. A 5-by-5 filter is used to smooth the small irregularities.

Input image G(x,y)	Binary image B (x,y)	Marker image N(x,y)																																																																																																												
<table><tr><td>155</td><td>133</td><td>134</td><td>54</td><td>42</td><td>42</td></tr><tr><td>116</td><td>136</td><td>67</td><td>42</td><td>42</td><td>39</td></tr><tr><td>36</td><td>76</td><td>66</td><td>36</td><td>42</td><td>41</td></tr><tr><td>34</td><td>33</td><td>52</td><td>43</td><td>40</td><td>40</td></tr><tr><td>38</td><td>33</td><td>130</td><td>115</td><td>40</td><td>37</td></tr><tr><td>32</td><td>31</td><td>34</td><td>43</td><td>44</td><td>50</td></tr></table>	155	133	134	54	42	42	116	136	67	42	42	39	36	76	66	36	42	41	34	33	52	43	40	40	38	33	130	115	40	37	32	31	34	43	44	50	<table><tr><td>1</td><td>1</td><td>1</td><td>0</td><td>0</td><td>0</td></tr><tr><td>1</td><td>1</td><td>0</td><td>0</td><td>0</td><td>0</td></tr><tr><td>0</td><td>0</td><td>0</td><td>0</td><td>0</td><td>0</td></tr><tr><td>0</td><td>0</td><td>0</td><td>0</td><td>0</td><td>0</td></tr><tr><td>0</td><td>0</td><td>1</td><td>1</td><td>0</td><td>0</td></tr><tr><td>0</td><td>0</td><td>0</td><td>0</td><td>0</td><td>0</td></tr></table>	1	1	1	0	0	0	1	1	0	0	0	0	0	0	0	0	0	0	0	0	0	0	0	0	0	0	1	1	0	0	0	0	0	0	0	0	<table><tr><td>155</td><td>133</td><td>134</td><td>0</td><td>0</td><td>0</td></tr><tr><td>116</td><td>136</td><td>0</td><td>0</td><td>0</td><td>0</td></tr><tr><td>0</td><td>0</td><td>0</td><td>0</td><td>0</td><td>0</td></tr><tr><td>0</td><td>0</td><td>0</td><td>0</td><td>0</td><td>0</td></tr><tr><td>0</td><td>0</td><td>130</td><td>115</td><td>0</td><td>0</td></tr><tr><td>0</td><td>0</td><td>0</td><td>0</td><td>0</td><td>0</td></tr></table>	155	133	134	0	0	0	116	136	0	0	0	0	0	0	0	0	0	0	0	0	0	0	0	0	0	0	130	115	0	0	0	0	0	0	0	0
155	133	134	54	42	42																																																																																																									
116	136	67	42	42	39																																																																																																									
36	76	66	36	42	41																																																																																																									
34	33	52	43	40	40																																																																																																									
38	33	130	115	40	37																																																																																																									
32	31	34	43	44	50																																																																																																									
1	1	1	0	0	0																																																																																																									
1	1	0	0	0	0																																																																																																									
0	0	0	0	0	0																																																																																																									
0	0	0	0	0	0																																																																																																									
0	0	1	1	0	0																																																																																																									
0	0	0	0	0	0																																																																																																									
155	133	134	0	0	0																																																																																																									
116	136	0	0	0	0																																																																																																									
0	0	0	0	0	0																																																																																																									
0	0	0	0	0	0																																																																																																									
0	0	130	115	0	0																																																																																																									
0	0	0	0	0	0																																																																																																									

Fig. 3 – The procedure to extract WBC edge pixels.

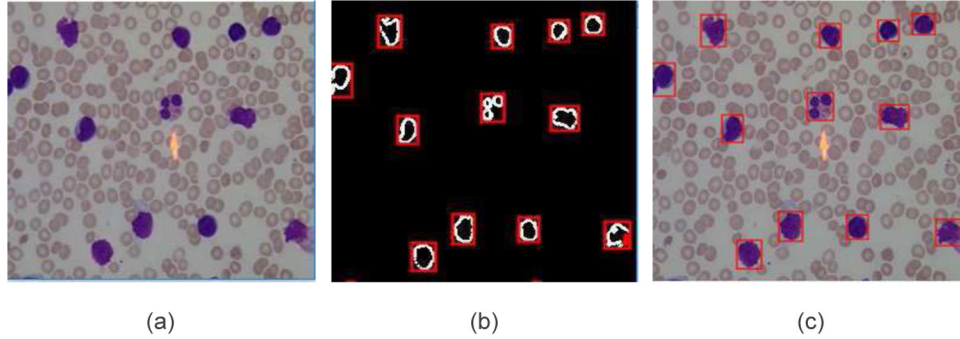

 Fig. 4 – The proposed edge strength-based location detection. *a* Input image. *b* Red windows contains WBC edge pixels. *c* WBC location windows.

Table 1 – Datasets.			
	Number	Resolution	Format
Cellavision	60	2864 × 2909	JPG
	1080	300 × 300	JPG
ALL-IDB	54	2592 × 1944	JPG
	130	1712 × 1368	JPG

Table 2 – Evaluation metrics.	
Measures	Formula
Recall	$\frac{TP}{TP+FN}$
Precision	$\frac{TP}{TP+FP}$
<i>f</i> -measure	$2 \cdot \frac{\text{Precision} \cdot \text{Recall}}{\text{Precision} + \text{Recall}}$

3. Datasets and evaluation metrics

The proposed method has been validated by the two datasets such as ALL-IDB¹ and Cellavision² datasets. The blood images were resized to 256 × 256 pixels because the actual image size is 2864 × 2909 and 2592 × 1944 pixels. The detailed information of these datasets is given in Table 1. The evaluation metrics is shown in Table 2. The variables from Table 2 are explained as follows: True Positive (TP) is a leukocyte region segmented as leukocyte region. True Negative (TN) is a non-leukocyte region segmented as non-leukocyte region. False Positive (FP) is a non-leukocyte region segmented as leukocyte region. False Negative (FN) is a leukocyte region segmented as non-leukocyte region. More description about these metrics has been reported by in [30]. All work was carried out in the MATLAB 2016a environment on a PC with an Intel Core i7 processor 3.60-GHz CPU and 14.0 GB of RAM running a Window 10 operating system (64-bit).

4. Experimental results

4.1. Leukocytes segmentation

The proposed leukocyte segmentation method was based on edge strength-based Grabcut approach. Fig. 5 illustrates the various segmented outputs of the sample image taken from the ALL-IDB dataset. Fig. 5(a) represents the input image from the ALL-IDB dataset and fuzzy clustering (FC) [31] output was shown in Fig. 5(b). The output obtained by the OTSU method [19] was illustrated in Fig. 5(c). The result yield by proposed segmentation method is shown in Fig. 5(d). The existing methods had false positives in segmented images. However, the proposed technique effectively removed false positives using threshold, which was identified from WBC edge pixels. According to Table 3, the proposed WBC segmentation algorithm produced a significantly improved segmentation performance in terms of precision, recall and *f*-measure compared to existing methods.

Based on Cellavision dataset, Fig. 6(a) illustrates the input image from Cellavision dataset. Fig. 6(b) represents the output of the C-OTSU method [32] and Fig. 6(c) shows the output of the FC technique [31]. Fig. 6(d) presents the obtained proposed method output. It was observed that the proposed algorithm

¹ <https://homes.di.unimi.it/scotti/all/>.

² <https://www.cellavision.com>.

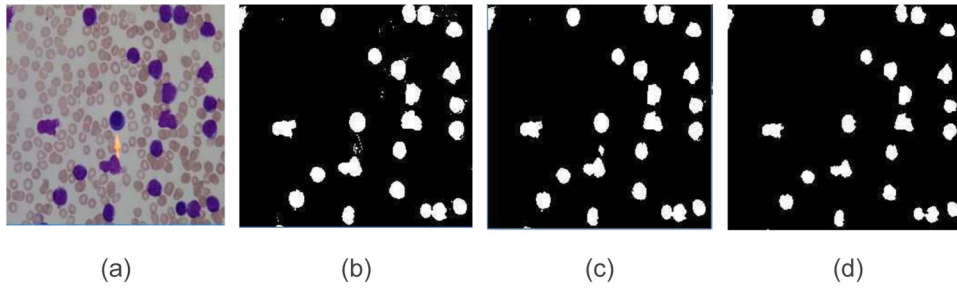


Fig. 5 – Segmentation comparison results on ALL-IDB dataset. a Original image. **b** FC method [31]. **c** OTSU method [19]. **d** Proposed segmentation method.

Table 3 – Quantitative analysis results of the proposed segmentation method with recent methods on ALL-IDB dataset.

Method	Precision	Recall	<i>f</i> -measure
OTSU [19]	0.8902	0.8234	0.8554
FC [31]	0.6008	0.6137	0.6071
Proposed method	0.9932	0.9805	0.9867

can remove non-leukocyte regions using gradient threshold value. From Table 4, the proposed method has been compared with competitor WBC segmentation algorithms including the neural architecture (NA) method [33], Color-based OTSU method [32], WBCs segmentation using k-means clustering [5], support vector regression (SVR) [17], adaptive location iteration-based Grabcut method [18], Otsu method [19] and FC technique [31]. As observed in Table 4, it confirmed that using the proposed method improved precision, recall and *f*-measure compared to the state-of-the-art techniques. Therefore, we have concluded that the proposed leukocyte segmentation method provided more accurate segmentation results. Additionally, comparison analysis on each cell type in WBC has been performed. Based on the experimental result analysis in Table 5, the proposed segmentation algorithm worked well on basophils, monocytes and lymphocytes.

4.2. Leukocytes counting

For counting analysis, only ALL-IDB dataset have been taken as the contained overlapped WBC regions in blood smear images. Fig. 7(a) represents the challenging blood smear images from

Table 4 – Quantitative analysis results of segmentation approaches on Cellavision dataset.

Year	Method	Precision	Recall	<i>f</i> -measure
2012	NA [33]	0.8534	0.7049	0.8001
2016	C-OTSU [32]	0.8981	0.7897	0.8459
2017	AIG [18]	0.9708	0.8786	0.9223
2018	K-Means [5]	0.9301	0.8123	0.8671
2018	SVR [17]	0.9655	0.8592	0.9242
2018	OTSU [19]	0.9781	0.8617	0.9161
2019	FC [31]	0.9025	0.8485	0.8746
	Proposed method	0.9963	0.8791	0.9341

ALL-IDB dataset. Fig. 7(b) illustrates the proposed segmentation method output. Red circles indicates the WBC region count using CHT method as shown in Fig. 7(c) and (d) represents the proposed GCHT method output and corresponding ground truth as shown in Fig. 7(e). It was observed that the proposed GCHT can count overlapped cell regions present in the blood smear image. Therefore, the proposed framework does not require any cell region separation techniques. Table 6 represents the comparison between the count obtained using the existing and proposed framework. It was noticed that the region count obtained using edge strength-based Grabcut with GCHT method was almost equal to expert's manual count. The existing methods produces more false positive region count in results. However, the proposed method eliminate false positive count using gradient threshold value in counting procedure in Section 2.4. The results proved that the proposed framework, that comprises of edge strength-based Grabcut and GCHT methods was efficient for counting the overlapped leukocyte regions.

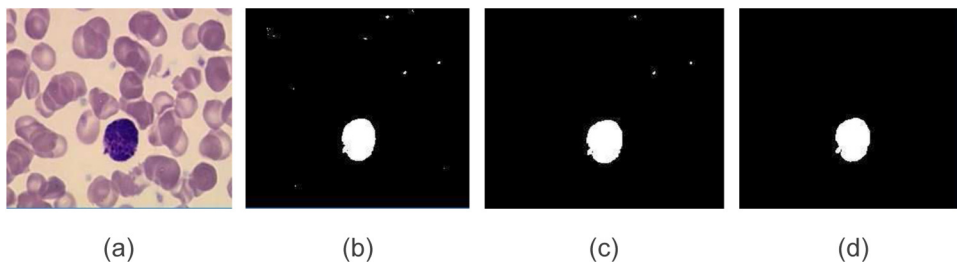
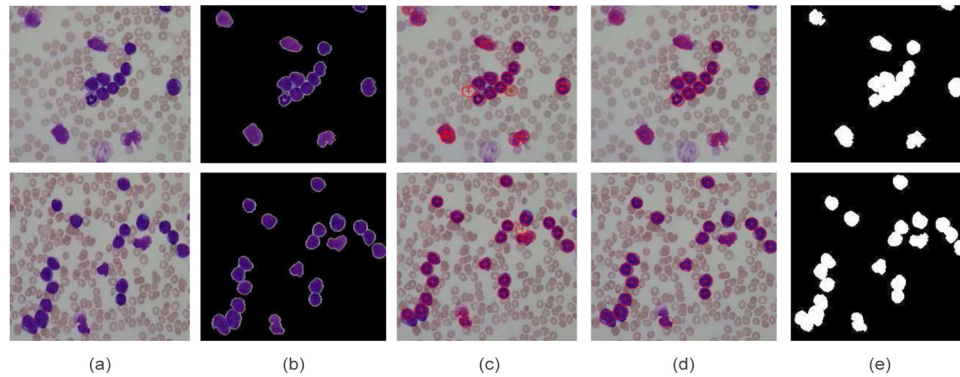


Fig. 6 – Segmentation comparison results on Cellavision dataset. a Original image. **b** C-OTSU method [32]. **c** FC method [31]. **d** Proposed segmentation method.

Table 5 – Different segmentation results comparison on each cell type in Cellavision dataset.

Cell types	No. of images	Precision	Recall	f-measure
<i>Cao et al. [17] ϵ-SVR based detection method</i>				
Basophils	13	0.9440	0.8359	0.8866
Eosinophils	11	0.9706	0.8418	0.9016
Neutrophils	9	0.9631	0.8567	0.9067
Lymphocytes	15	0.9601	0.8542	0.9040
Monocytes	12	0.9899	0.8777	0.9304
Mean		0.9655	0.8532	0.9058
<i>Liu et al. [18] Adaptive location and Grabcut</i>				
Basophils	13	0.9605	0.8393	0.8958
Eosinophils	11	0.9982	0.8481	0.9170
Neutrophils	9	0.9870	0.8531	0.9151
Lymphocytes	15	0.9680	0.8659	0.9141
Monocytes	12	0.9956	0.8895	0.9395
Mean		0.9818	0.8592	0.9163
<i>Alferez et al. [31] Fuzzy clustering</i>				
Basophils	13	0.9590	0.8458	0.8988
Eosinophils	11	0.9816	0.8408	0.9057
Neutrophils	9	0.9773	0.8634	0.9168
Lymphocytes	15	0.9770	0.8704	0.9206
Monocytes	12	0.9959	0.8884	0.9390
Mean		0.9781	0.8617	0.9161
<i>Proposed edge strength-based Grabcut method</i>				
Basophils	13	0.9998	0.8999	0.9482
Eosinophils	11	0.9957	0.8615	0.9237
Neutrophils	9	0.9873	0.8602	0.9193
Lymphocytes	15	0.9999	0.8844	0.9386
Monocytes	12	0.9989	0.8895	0.9410
Mean		0.9963	0.8791	0.9341


Fig. 7 – Leukocytes overlapped region counting results on ALL-IDB dataset. a Original image. b Output of proposed segmentation method. c Output of CHT method. d Output of GCHT technique. e Ground truth.

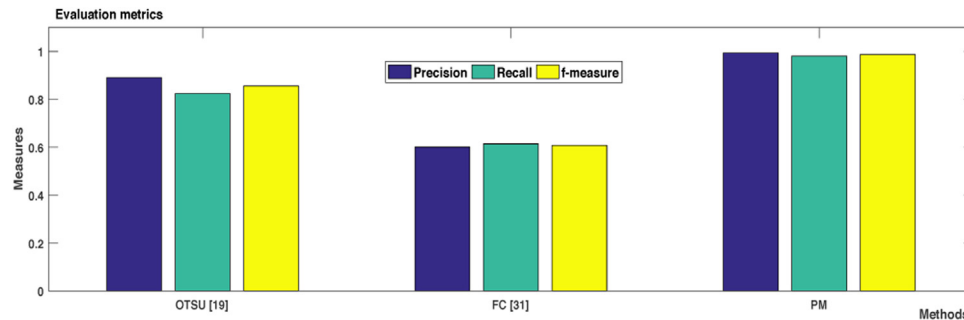
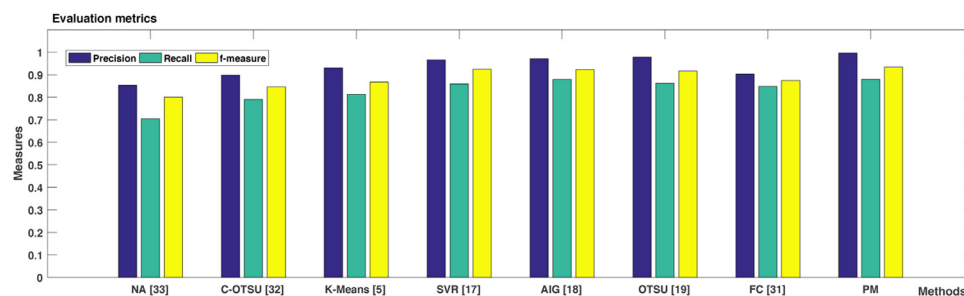
5. Discussion

Since the inspection of leukocytes in microscopic blood image can assist doctors to diagnose diseases, the proposed framework can segment leukocytes based on edge strength-based Grabcut and count leukocytes using the GCHT algorithm. There were instances where existing methods produces many false positive WBC regions, e.g., Figs. 5 and 6. From the

qualitative analysis, it was observed the high dependence of the methods in [19] and [31] on its parameter T and cluster size, whereas the method proposed in this paper produced consistent results. Another strength of the proposed method was that even when the overlapped regions appear in datasets, the WBCs segmentation performance was not compromised, as depicted in Figs. 8 and 9. Additionally, the proposed framework does not have further need of the cell region separation procedure. From Fig. 7, it is observed that the GCHT method was able to count even overlapped cell regions present

Table 6 – Comparison between existing count and count obtained by GCHT method on ALL-IDB dataset.

Segmentation method	Counting method	Total count	Manual count
OTSU [19]	CHT	210	182
Edge strength-Grabcut	CHT	201	182
Edge strength-Grabcut	GCHT	177	182

**Fig. 8 – Segmentation performance comparison with the recent state-of-the-art methods on ALL-IDB dataset.****Fig. 9 – Segmentation performance comparison with the state-of-the-art methods on Cellavision dataset. Please note: NA-neural architecture, C-OTSU-color OTSU method, SVR-support vector regression, AIG-adaptive iteration grabcut, OTSU-OTSU threshold method, FC-fuzzy clustering, PM-proposed method.**

in blood smear image. In Table 6, the region count obtained by proposed framework was better compared to the existing methods. This success was attributed to better segmentation based on edge strength-based Grabcut and GCHT method. From experimental results, the proposed approach obtained a good solution to increase leukocytes counting accuracy than the state-of-the-art techniques. The obtained results proved that the S component produced best outcomes of leukocytes segmentation in microscopic images than the other components. Lastly, the proposed framework does not require iteration, so it took a minimum cost time of 7.40 s.

6. Conclusion

This paper proposed a novel leukocytes counting framework, which employs an edge strength-based Grabcut method and GCHT technique. First, the leukocytes were segmented based on the edge strength-based Grabcut method. Further, the GCHT algorithm was applied to find the leukocyte region count in blood smear images. The proposed edge strength location

detection can be used to avoid bad influences of background elements such as platelets, RBCs, and plasma. The proposed segmentation method can segment any complex internal characteristics of cells. Experimental results obtained from ALL-IDB and Cellavision datasets depict that our method significantly outperforms the existing leukocytes segmentation methods with higher recall, precision, and f -measure rates. Moreover, the proposed framework can segment and count leukocytes even when complex cell regions present in datasets. The use of leukocytes counting can be helpful for the pathologists in hospitals.

Conflict of interest

The authors declare that they have no conflict of interest.

Human and animal rights

This study did not involve human participants and animals.

Acknowledgements

This research has been supported by the Anna University, Chennai and the Anna Centenary Research Fellowship (ACRF) has been granted towards the conduct of this research.

REFERENCES

- [1] Sajjad M, Khan S, Jan Z, Muhammad K, Moon H, Kwak JT, et al. Leukocytes classification and segmentation in microscopic blood smear: a resource-aware healthcare service in smart cities. *IEEE Access* 2017;5:3475–89. <http://dx.doi.org/10.1109/ACCESS.2016.2636218>
- [2] Ghane N, Vard A, Talebi A, Nematollahy P. Segmentation of white blood cells from microscopic images using a novel combination of k-means clustering and modified watershed algorithm. *J Med Signals Sens* 2017;7(2):92–101. <http://dx.doi.org/10.4103/2228-7477.205503>
- [3] Negm AS, Hassan OA, Kandil AH. A decision support system for acute leukaemia classification based on digital microscopic images, vol. 54. Elsevier; 2017. <http://dx.doi.org/10.1016/j.aej.2017.08.025>
- [4] Ferdosi BJ, Nowshin S, Sabera FA. White blood cell detection and segmentation from fluorescent images with an improved algorithm using k-means clustering and morphological operators. 2018 4th International Conference on Electrical Engineering and Information & Communication Technology (ICEEICT); 2018. pp. 566–70. <http://dx.doi.org/10.1109/CEEICT.2018.8628068>
- [5] Zheng X, Wang Y, Wang G, Liu J. Fast and robust segmentation of white blood cell images by self-supervised learning. *Micron* 2018;107:55–71. <http://dx.doi.org/10.1016/j.micron.2018.01.010>
- [6] Cao H, Liu H, Song E. Bone marrow cells detection: a technique for the microscopic image analysis. *J Med Syst* 2019;42(82):1–14. <http://dx.doi.org/10.1007/s10916-019-1185-9>
- [7] Rawat J, Singh A, Bhadauria H, Virmani J, Devgun JS. Computer assisted classification framework for prediction of acute lymphoblastic and acute myeloblastic leukemia. *Biocybern Biomed Eng* 2017;37(4):637–54. <http://dx.doi.org/10.1016/j.bbe.2017.07.003>
- [8] Mishra S, Majhi B, Sa PK. Texture feature based classification on microscopic blood smear for acute lymphoblastic leukemia detection. *Biomed Signal Process Control* 2019;47:303–11. <http://dx.doi.org/10.1016/j.bspc.2018.08.012>
- [9] Hegde RB, Prasad K, Hebbar H, Singh BMK. Development of a robust algorithm for detection of nuclei of white blood cells in peripheral blood smear images. *Multim Tools Appl* 2019;42(6):1–20. <http://dx.doi.org/10.1007/s10916-018-0962-1>
- [10] Wang Y, Cao Y. Leukocyte nucleus segmentation method based on enhancing the saliency of saturation component. *J Algorithms Comput Technol* 2019;13:1–10. <http://dx.doi.org/10.1177/1748302619845783>
- [11] Rawat J, Singh A, Bhadauria H, Virmani J, Devgun J. Leukocyte classification using adaptive neuro-fuzzy inference system in microscopic blood images. *Arab J Sci Eng* 2018;43(12):7041–58.
- [12] Moshavash Z, Danyali H, Helfroush MS. An automatic and robust decision support system for accurate acute leukemia diagnosis from blood microscopic images. *J Digit Imaging* 2018;31(5):1–16. <http://dx.doi.org/10.1007/s10278-018-0074-y>
- [13] Supriyanti R, Satrio G, Ramadhani Y, Siswandari W. Contour detection of leukocyte cell nucleus using morphological image. *J Phys Conf Ser* 2017;824:012069. <http://dx.doi.org/10.1088/1742-6596/824/1/012069>. IOP Science
- [14] Wang Q, Chang L, Zhou M, Li Q, Liu H, Guo F. A spectral and morphologic method for white blood cell classification. *Optics Laser Technol* 2016;84:144–8. <http://dx.doi.org/10.1016/j.bspc.2018.08.012>
- [15] Chaira T. Accurate segmentation of leukocyte in blood cell images using atanassov's intuitionistic fuzzy and interval type ii fuzzy set theory. *Micron* 2014;61:1–8. <http://dx.doi.org/10.1016/j.micron.2014.01.004>
- [16] Duan Y, Wang J, Hu M, Zhou M, Li Q, Sun L, et al. Leukocyte classification based on spatial and spectral features of microscopic hyperspectral images. *Optics Laser Technol* 2019;112:530–8. <http://dx.doi.org/10.1016/j.optlastec.2018.11.057>
- [17] Cao F, Liu Y, Huang Z, Chu J, Zhao J. Effective segmentations in white blood cell images using ϵ -svr-based detection method. *Neural Comput Appl* 2019;31:6767–80. <http://dx.doi.org/10.1007/s00521-018-3480-7>
- [18] Liu Y, Cao F, Zhao J, Chu J. Segmentation of white blood cells image using adaptive location and iteration. *IEEE J Biomed Health Inform* 2017;21(6):1644–55. <http://dx.doi.org/10.1109/JBHI.2016.2623421>
- [19] Safuan SNM, Tomari MRM, Zakaria WNW. White blood cell (wbc) counting analysis in blood smear images using various color segmentation methods. *Measurement* 2018;116:543–55. <http://dx.doi.org/10.1016/j.measurement.2017.11.002>
- [20] Wang Y, Cao Y. Quick leukocyte nucleus segmentation in leukocyte counting. *Comput Math Methods Med* 2019;1–10. <http://dx.doi.org/10.1155/2019/3072498>
- [21] Gomolka RS, Korzynska A, Siemion K, Gabor-Siatkowska K, Klonowski W. Automatic method for assessment of proliferation index in digital images of dlbc tissue section. *Biocybern Biomed Eng* 2019;39(1):30–7. <http://dx.doi.org/10.1016/j.bbe.2018.09.004>
- [22] Wang Q, Bi S, Sun M, Wang Y, Wang D, Yang S. Deep learning approach to peripheral leukocyte recognition. *PLOS ONE* 2019;14(6):1–18. <http://dx.doi.org/10.1371/journal.pone.0218808>
- [23] Fan H, Zhang F, Xi L, Li Z, Liu G, Xu Y. Leukocytemask: an automated localization and segmentation method for leukocyte in blood smear images using deep neural networks. *J Biophotonics* 2019;12(7):1–14. <http://dx.doi.org/10.1002/jbio.201800488>
- [24] Zhao J, Zhang M, Zhou Z, Chu J, Cao F. Automatic detection and classification of leukocytes using convolutional neural networks. *Med Biol Eng Comput* 2017;55(8):1287–301. <http://dx.doi.org/10.1007/s11517-016-1590-x>
- [25] Di Ruberto C, Loddio A, Putzu L. A leucocytes count system from blood smear images. *Mach Vis Appl* 2016;27(8):1151–60. <http://dx.doi.org/10.1007/s00138-016-0812-4>
- [26] Loddio A, Putzu L, Di Ruberto C, Fenu G. A computer-aided system for differential count from peripheral blood cell images. 2016 12th International Conference on Signal-Image Technology & Internet-Based Systems (SITIS). 2016. pp. 112–8. <http://dx.doi.org/10.1109/SITIS.2016.26>
- [27] Porcu S, Loddio A, Putzu L, Di Ruberto C. White blood cells counting via vector field convolution nuclei segmentation. *Proceedings of the 13th International Joint Conference on Computer Vision, Imaging and Computer Graphics Theory*

- and Applications; 2018. p. 227–34.
<http://dx.doi.org/10.5220/0006723202270234>
- [28] Zheng X, Wang Y, Wang G, Chen Z. A novel algorithm based on visual saliency attention for localization and segmentation in rapidly-stained leukocyte images. *Micron* 2014;56:17–28.
<http://dx.doi.org/10.1016/j.micron.2013.09.006>
- [29] Rother C, Kolmogorov V, Blake A. Grabcut: interactive foreground extraction using iterated graph cuts. *ACM transactions on graphics (TOG)*, vol. 23. ACM; 2004. p. 309–14.
<http://dx.doi.org/10.1145/1186562.1015720>
- [30] Taha AA, Hanbury A. Metrics for evaluating 3d medical image segmentation: analysis, selection, and tool. *BMC Med Imaging* 2015;15(1):1–29.
<http://dx.doi.org/10.1186/s12880-015-0068-x>
- [31] Alférez S, Merino A, Acevedo A, Puigví L, Rodellar J. Color clustering segmentation framework for image analysis of malignant lymphoid cells in peripheral blood. *Med Biol Eng Comput* 2019;57(6):1–19.
<http://dx.doi.org/10.1007/s11517-019-01954-7>
- [32] Tareef A, Song Y, Cai W, Wang Y, Feng DD, Chen M. Automatic nuclei and cytoplasm segmentation of leukocytes with color and texture-based image enhancement. *IEEE 13th International Symposium on Biomedical Imaging (ISBI)*; 2016. pp. 935–8.
<http://dx.doi.org/10.1109/ISBI.2016.7493418>
- [33] Mohapatra S, Patra D, Kumar S, Satpathy S. Lymphocyte image segmentation using functional link neural architecture for acute leukemia detection. *Biomed Eng Lett* 2012;2:100–10.
<http://dx.doi.org/10.1007/s13534-012-0056-9>